RSC Advances

ROYAL SOCIETY OF CHEMISTRY

www.rsc.org/advances

Graphical Abstract

CS-PWA/Nafion composite membranes were successfully synthesized via Layer-by-layer self-assembly technique, exhibiting low vanadium ion permeability and improved comprehensive performance in VRFB.

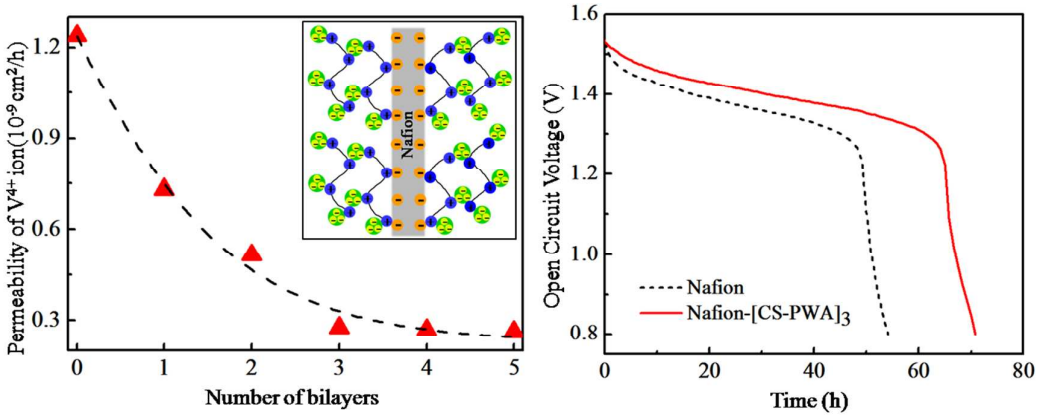

Layer-by-layer self-assembly of Nafion-[CS-PWA] composite membranes with suppressed vanadium ion crossover for vanadium redox flow battery applications

Shanfu Lu[a, b], Chunxiao Wu[a, b], Dawei Liang[a, b], Qinglong Tan[a, b], Yan Xiang[a, b, *]

[a] *Beijing Key Laboratory of Bio-inspired Energy Materials and Devices, School of Chemistry and Environment, Beihang University, Beijing, 100191, P. R. China.*

[b] *Key Laboratory of Bio-Inspired Smart Interfacial Science and Technology of Ministry of Education, School of Chemistry and Environment, Beihang University, Beijing, 100191, P.R. China*

[*] Address correspondence to xiangy@buaa.edu.cn

Abstract: A novel polymer-inorganics composite membrane, Nafion-$[CS\text{-}PWA]_n$ (n= the number of multilayer), was prepared by layer-by-layer self-assembly technique with polycation chitosan (CS) and negatively charged phosphotungstic acid (PWA) for vanadium redox flow battery applications. The UV-visible spectra and SEM results showed that CS-PWA multilayer was successfully fabricated on the surface of Nafion membrane, and FTIR result showed that there was a strong interaction between the CS and PWA molecules. The obtained Nafion-$[CS\text{-}PWA]_n$ showed much lower vanadium ion permeability compared with pristine Nafion membrane. Accordingly, the VRFB with Nafion-$[CS\text{-}PWA]_3$ membrane exhibited higher coulombic efficiency (CE) and energy efficiency (EE) together with a slower self-discharge rate than that of pristine Nafion212 system.

1. Introduction

Flow battery (FB) system has been extensively studied as a clean and efficient power source for applications in energy storage system[1], and it becomes a valid solution to solve the energy shortages[2, 3]. Among its several systems such as

polysulfide/bromide, iron/chromium, etc, with the advantages of the abundant of vanadium resource and the low cost, as well as high energy efficiency, long lifetime, fast response time, deep-discharge capacity [4], vanadium redox flow battery (VRFB) has recently attracted considerable research interest[5-9].

The ion exchange membrane (IEM) is one of the key materials in VRFB system. It functions as a separator of the cathode and anode compartments to prevent their crossover and allows the transport of proton to maintain the electrical balance during the charge-discharge process. Therefore, an ideal IEM that exhibits high proton conductivity and good stability, as well as outstanding ion selectivity is critically important for commercializing VRFB[8-11]. State-of-the-art IEM in VRFBs is perfluorosulfonic acid cation exchange membranes, such as Nafion membrane (DuPont, America), exhibiting high conductivity, chemical and mechanical stability. However, the high vanadium ion permeability of Nafion affect its further application and development in VRFB[12]. The crossover of vanadium ions through proton-exchange membrane is the chief reason that results in high self-discharge rate and then lead to a low coulombic efficiency (CE), energy efficiency (EE). To solve this problem, many researches had pay attention to the modification of Nafion membrane, such as, blending with PVDF to prepare Nafion-PVDF composite membrane[13], recasting with inorganic nanoparticles to form Nafion-SiO_2 membranes[14, 15], oxidation polymerizing or electrodepositing polymer on the surface of Nafion[16]. All of above modification methods can be used to decrease the crossover of vanadium ions in Nafion membrane, and in general, improves the cell performance of VRFB [14]. However, the incorporation of inorganic nanoparticles or polymers inevitably alters the microstructure of Nafion, resulting in deterioration in mechanical properties.

The layer-by-layer (LbL) self-assembly technique is an efficient method for fabricating multilayer thin films with controlled architecture and composition at the nanometer scale [17]. It does not become public until this technique was rediscovered by Decher and Hong [18] in 1992, but recently years it has been widely used in new energy

materials to prepare polymer/polymer layers onto the membrane surface, and find that it has a significant influence on ion selectivity and the cell with these membranes display high efficiency[14, 19, 20]. Previously, our group has been introduced the inorganic compound PWA, a well known super proton conductor, to prepare a composite membrane by the self-assembly technique in DMFC to suppress methanol crossover and maintain high proton conductivity of the membrane , consequently, the cell with the self-assembled membrane achieves a good cell performance [21,22].

The heteropoly acids (HPAs) are well known superionic conductor in their fully hydrated states [23]. Among the Keggin-type HPAs phosphotungstic acid ($H_3PW_{12}O_{40}$, PWA) has the strongest acidity and proton conductivity. Here, we used the LbL self-assembly technique to trap and anchor PWA molecules on the Nafion membrane surface for vanadium redox flow battery application. The self-assembled CS-PWA bilayers not only suppress the vanadium ion crossover but also minimise the impact on the proton conductivity of the Nafion membranes. VRFB with the self-assembled Nafion-$[CS\text{-}PWA]_n$ membrane show higher coulombic efficiency (CE) and energy efficiency (EE) together with a slower self-discharge rate than that with pristine Nafion212 system.

2. Experimental

2.1 Materials

Chitosan (M_w=60000, CS, Hai Debei) and $H_3PW_{12}O_{40}$ (PWA, Aldrich-Sigma) were used without further treatment. Nafion212 membranes were purchased from DuPont. Prior modification, Nafion membranes were treated according to the standard procedure which was 30 min in 3 wt% H_2O_2 solution at 80 ^oC, and rinsed with Milli-Q water for 5 times, and then 30 min in 0.5 M H_2SO_4 solution at 80 ^oC, finally stored in Milli-Q water.

2.2 Preparation of Nafion-$[CS\text{-}PWA]_n$ membrane

The Layer-by-Layer (LBL) self-assembled CS-PWA multilayer was carried out by alternate immersing the pretreated Nafion membrane in CS acetic acid solution (2 wt%) and PWA ethanol solution (20 mM) at room temperature for 15 min. After each immersing step, the membrane was rinsed with Milli-Q water to remove the free CS and PWA on the surface. The process of alternative immersing in CS and PWA solution was then repeated to increase the number of multilayer. The resulting poly-electrolyte multilayer modified composite membrane was denoted as Nafion-$[CS\text{-}PWA]_n$, and they were finally stored in Milli-Q water before use. The schematic of LBL self-assembled Nafion-$[CS\text{-}PWA]_n$ membrane was as followed (Fig.1).

2.3 Membrane characterization

The formation of LbL self-assembled multilayers on the membrane effectively prepared from polyelectrolytes was monitored by a GBC Cintra 10e series UV-vis spectroscopy. During the test, Milli-Q water was used as a blank for calibration of the instrument and then measuring the absorption spectrum of membranes at room temperature. Fourier Transform Infrared Spectroscopy (FT-IR) was used to judge the interaction between the functional groups on chitosan and PWA.

The cross-sectional structure of the multilayer membranes was sputtered with gold and measured using a JEOL JSM-5800 scanning electronic microscope (SEM) at an acceleration voltage of 5 KV and a energy dispersive X-ray spectrometer (EDX). The samples were prepared by freezing the membranes in liquid nitrogen followed by breaking the frozen membrane with forceps. In addition, surface roughness and morphology of the composite membranes were conducted with atomic force microscope (AFM) using a Dimension Icon instrument (Bruker ,USA).

Proton conductivity (σ) was measured using a four-point probe electrochemical impedance spectroscopy technique over a frequency range of 1 Hz to 100 kHz using a Princeton Applied Research PARSTAT 2273 potentiostat/galvanostat. The membrane was fixed between two half-cells with 1 M $VOSO_4$/3 M H_2SO_4 solution. The

resistances with and without membrane were measured, recorded as R_1 and R_2, respectively. Specially, in this work, each result had been measured five times, and then taking the average in the eventually calculation. The transverse resistance R (Ω) and the conductivity σ (S.cm^{-1}) can be calculated using the following equation: [24]

$$R=R_2-R_1 \quad (1)$$

$$\sigma=\frac{L}{R\times S} \quad (2)$$

where S was the electrode area ,and L was the thickness of the membrane.

Permeability of vanadium ion was determined by measuring the diffusion of VO^{2+}. The membrane was exposed in a solution of 1 M $VOSO_4$/3 M H_2SO_4 on the left reservoir and a solution of 1 M $MgSO_4$/3 M H_2SO_4 on the right reservoir. $MgSO_4$ solution was just used to equalize the ionic strengths of the two sides so as to minimize the effects of osmotic pressure [25]. Samples of the solution from the right reservoir were taken out at a regular time intervals and were used to measure the concentration of VO^{2+} by UV-vis spectroscopy. Accordingly, the vanadium ion concentration as a function of time is given by the equation [26]:

$$V_B\frac{dC_B(t)}{dt}=A\frac{P}{L}(C_A-C_B(t)) \quad (3)$$

Where C_A was the vanadium ion concentration in the left reservoir, and $C_B(t)$ refers to the vanadium ion concentration in the right reservoir as a function of time. A and L were electrode area (cm^2) and thickness (cm) of the membrane. P was the permeability of vanadium ions, and V_B was the volume of the right reservoir.

VRFB single cell performance was characterized by conducting with 1 M $VOSO_4$/ 3 M H_2SO_4 solution as the anolyte and 1 M V^{3+} /3 M H_2SO_4 as the catholyte. Membrane thickness for all tests was 56-60 μm and the electrode area was 4 cm^2. The coulombic efficiency (CE), voltage efficiency (VE) and energy transfer efficiency (EE) were calculated as follows [26],

$$CE=\frac{\int I_d dt}{\int I_c dt}*100\% \quad (4)$$

$$EE=\frac{\int V_d I_d dt}{\int V_c I_c dt}*100\% \quad (5)$$

$$VE=\frac{EE}{CE}*100\% \quad (6)$$

Where I_d and I_c were discharging and charging current, V_d and V_c were discharging and charging voltage, respectively.

3. Results and discussion

3.1 Membrane characterization

Fig.2a shows UV-vis spectra of the LbL self-assembled Nafion212 membranes as a function of the number of CS-PWA bilayers. UV-vis spectra of the membranes exhibites a characteristic absorption peak at 265 nm and increases with an increasing number of the self-assembled CS-PWA bilayers. PWA has a characteristic absorption peak at 265 nm, while CS is basically transparent in the UV-vis spectral range. Thus, the increase in the absorbance at 265 nm is attributed to the adsorption of PWA molecules on the previously deposited CS-PWA multilayer. The inset graph of Fig.2a depicts the absorbance at 265 nm as a function of the number of CS-PWA bilayers, which increase linearly with the number of assembled CS-PWA multilayer. This linearly relationship indicates that a same amount of polymer was deposited in every dipping cycle.

To verify the interaction between CS and PWA of self-assembled multilayer on Nafion surface, FTIR was used to analysis the membrane. Fig.2b shows FTIR spectrum of pure PWA, CS and Nafion-$[CS\text{-}PWA]_3$ membrane. For pure PWA, characteristic bands are observed at 890 cm^{-1} (W-O_b-W), 983.9 cm^{-1} (W=O_d), 893.9 cm^{-1} (W-O_b-W) and 803.9 cm^{-1} (W-O_c-W), which coincide with the reported in the reference for the $[PW_{12}O_{40}]^{3-}$ Keggin unite structure[27]. Compared with pure PWA, the corresponding peaks of the membrane exhibit an obviously blue shift, which indicate that the terminal oxygen atom of PWA strongly interacted with the hydroxy group and the amino group of chitosan. To further confirm the strong interaction between PWA and CS, we mixed CS solution with PWA solution and found that there formed a large amount of white precipitate immediately. The result indicate that there indeed

exist a strong interaction between PWA and CS, which ensure that the PWA molecules trapped in the CS-PWA bilayer don't leached out in aqueous solution.

The morphology and topography of the pristine Nafion membrane and the assembled Nafion-[CS-PWA]$_3$ membrane were measured by AFM and SEM, showing in Fig. 3. Based on the AFM image (Fig.3a and 3b), it is obviously characterized that the assembled Nafion-[CS-PWA]$_3$ membrane shows distributed spikes, while the surface of the pristine Nafion membrane is smooth and flat. The mean interface roughness (R_a) of the pristine Nafion membrane and Nafion-[CS-PWA]$_3$ are 0.38 nm and 5.18 nm, respectively. It indicate that something presence on the surface of Nafion membrane. In order to identify CS-PWA multilayer has changed the roughness, we analyzed the membrane cross-section by using SEM. Fig. 3c is the SEM image of the 18 CS-PWA multilayer self-assembled membrane cross-section. The image clearly shows that the dense, homogenous multilayer is formed on the side of Nafion membrane. The thickness of CS-PWA multilayer is about 1.2 μm. It can be calculated that each CS-PWA layer is about 60-70 nm. Furthermore, the EDX (Fig. 3d and 3e) indicate that element fluorine uniformly distribute within the Nafion membrane and tungsten exist in the self-assembled multilayer. Specially, the results of the AFM and SEM make a well consistent with the FTIR and UV-vis results.

3.2 Proton conductivity and vanadium ion permeability

The proton conductivity and the diffusion coefficient of V(IV) ions of the self assembled Nafion-[CS-PWA]$_n$ membrane were measured at room temperature. As show in Fig.4a, the conductivities of the assembled Nafion-[CS-PWA]$_n$ membrane are all lower than that of pristine Nafion membrane (0.129 S.cm^{-1}) in 1 M $VOSO_4$/3 M H_2SO_4. With the increase of the self-assembled CS-PWA bilayer, proton conductivity of the membranes decrease gradually, probably due to the incorporated proton conducting PWA in the multilayer structure as CS in the multilayer structure would not contribute to the conductivity. Fig. 4b shows the vanadium ion permeability of the Nafion-[CS-PWA]$_n$ membranes as a function of self-assembled CS-PWA bilayer.

Compared with the conductivity, the vanadium ion permeability decrease sharply with the increasing number of bilayer. However, after the self-assembled CS-PWA bilayer up to 3, there is little change in the vanadium ion permeability of the membranes, indicating that the self-assembled CS-PWA bilayer has reached their limit to block the vanadium crossover.

As the literature[13] reported, Nafion membrane had a dual structure with a hydrophobic region interspersed with ion-rich hydrophilic domains, and a hydrophilic water-rich domains associated with $-SO_3$ polar clusters on the surface which formed a channel. The proton could across the membrane through the channel to maintain a high proton conductivity. However, hydrated V(IV) (bonding with sulfonic acid groups) combined with water molecules can also enter the channel, which then traverse to the other side. Exactly as we expected, self-assembled of CS-PWA bilayer on the surface of Nafion membrane not only can effectively suppress the crossover of V(IV) ion but also minimise the impact on the proton conductivity of Nafion membranes.

Since IEM applied in VRFB should possess simultaneously high proton conductivity and low vanadium ion permeability, a new parameter, selectivity (the ratio of proton conductivity to ion permeability, σ/P), is defined to compare the comprehensive character of the composite membranes. That is to say, the higher value of the σ/P, the better the performance of the membrane. Fig. 4b is the plot of σ/P of Nafion212 membrane as a function of the number of self-assembled CS-PWA bilayer. As shown in the graph, the σ/P ratio reaches a maximum value of 2.2×10^7 S.h.cm^{-3} for the composite membrane with 3 self-assembled CS-PWA bilayers and was about 2 times higher than that of any other membranes. Hence, we applied the Nafion-$[CS\text{-}PWA]_3$ self-assembled membrane to the following tests.

3.3 Single cell performance

Charge-discharge curves of the VRFB with Nafion and Nafion-$[CS\text{-}PWA]_3$ membrane at current density of 30-60 mA/cm^2 are shown in Fig.5. Results indicate

that the charge-discharge voltage platform and capacity of VRFB with Nafion-[CS-PWA]$_3$ membrane are both better than that with pristine Nafion212. This is owing to the integrated effect of membrane conductivity and vanadium ion permeability. Although low conductivity will not be good for charge-discharge process, less decline the of vanadium ion permeability result in a better charge-discharge performance of composite membrane than that of pristine Nafion212. As shown in Fig.6, the CE, VE and EE of VRFB with Nafion-[CS-PWA]$_3$ membrane at various charge-discharge current densities are better than of that with Nafion212. In the case of VRFB with Nafion membrane, vanadium ions will crossover through the Nafion membrane during the charge-discharge process and react with those vanadium ions which have different valence state, resulting in a lower CE and EE. But for the VRFB with Nafion-[CS-PWA]$_3$ membrane, the transporting of vanadium ions through the membrane has been greatly reduced. And hence, a relatively high CE and EE can be achieved.

Open circuit voltage (OCV) is an important parameter for the self-discharge of VRFB single cell. Self-discharge of VRFB is mainly due to the crossover of vanadium ion through the membrane between the positive reservoir and negative reservoir. VRFB self-discharge with different membrane was characterized by monitoring the OCV at room temperature after it was charged to a state of charge (*SOC*) of 80%. As show in Fig.7, OCV value decreases slowly with storage time at the beginning and then drop sharply to 0.8 V. The maintaining time of OCV above 1.3 V of VRFB with Nafion-[CS-PWA]$_3$ membrane is 70 h which longer than that with pristine Nafion (50 h). This result is in good accordance with the vanadium ion permeability result, indicating that the Nafion-[CS-PWA]$_3$ composite membrane exhibits an excellent performance for VRFB applications.

In order to evaluate the stability of the self-assembled membrane under the working condition of VRFB, the single cell with Nafion-[CS-PWA]$_3$ or Nafion membrane was cycled at the current density of 60 mA/cm^2 and the result was presented in Fig. 8. During 35 cycles, the CE and EE of the VRFB with Nafion-[CS-PWA]$_3$ membrane

are all higher than that with Nafion membrane, which attributed to the lower vanadium permeability of assembled Nafion membrane. The efficiency of the VRFB with the assembled Nafion-$[CS\text{-}PWA]_3$ membrane does not tend to decline during 35 cycles, indicating that the self-assembled membrane possess good stability in vanadium electrolyte under the working condition, thus is able to maintain an excellent comprehensive cell performance.

4. Conclusion

In this work, Nafion-$[CS\text{-}PWA]_n$ membranes were successfully prepared by layer-by-layer self-assembly technique on Nafion surface with chitosan and PWA. The self-assembled CS-PWA bilayer were confirmed by AFM, SEM, FTIR and UV-vis spectrum. The self-assembled CS-PWA bilayer not only suppress the vanadium ion crossover but also minimise the impact on the proton conductivity of the Nafion membrane. When three CS-PWA bilayers were assembled, the selectivity (σ/P) of the composite membrane reached a max value. The VRFB single cell with Nafion-$[CS\text{-}PWA]_3$ membrane showed higher coulombic efficiency, energy efficiency and lower self-discharge rate than that with pristine Nafion membrane. As a result, the self-assembled Nafion-$[CS\text{-}PWA]_n$ membrane was a potential ion exchange membrane for VRFB application.

Acknowledgments

This work was financially supported by grants from the National Natural Science Foundation of China (No.21003007, U1137602, 21073010), National High Technology Research and Development Program of China (863 program, 2013AA031902), National Program on Key Basic Research Project (973 Program) (No.2011CB935700), National Science Foundation of Beijing (No. 2132051), Beijing Higher Education Young Elite Teacher Project (No.29201493) and the Fundamental Research Funds for the Central Universities (YWF-13-T-RSC-030).

References

1 C. Ding, H. Zhang, X. Li, T. Liu and F. Xing, *J.Phys.Chem.Lett.* 2013, 4, 1281-1294.

2 B. Dunn, H. Kamath and J. M. Tarascon, *Science*, 2011, 334, 928-935.

3 G. L. Soloveichik, in *Annual Review of Chemical and Biomolecular Engineering*, Vol 2, ed. J. M. Prausnitz, 2011, vol. 2, pp. 503-527.

4 M. Skyllas-Kazacos, M. H. Chakrabarti, S. A. Hajimolana, F. S. Mjalli and M. Saleem, *Journal of The Electrochemical Society*, 2011, 158, R55.

5 B. Schwenzer, J. Zhang, S. Kim, L. Li, J. Liu and Z. Yang, *ChemSusChem*, 2011, 4, 1388-1406.

6 M. Skyllas-Kazacos, M. Rychcik, R. G. Robins, A. Fane and M. Green, *J. Electrochem. Soc.;(United States)*, 1986, 133.

7 E. Sum, M. Rychcik and M. Skyllas-Kazacos, *J. Power sources*, 1985, 16, 85-95.

8 C. Fabjan, J. Garche, B. Harrer, L. Jörissen, C. Kolbeck, F. Philippi, G. Tomazic and F. Wagner, *Electrochim. Acta*, 2001, 47, 825-831.

9 T. Mohammadi and M. Skyllas-Kazacos, *J.Membr. Sci.* 1995, 107, 35-45.

10 W. Wang, Q. Luo, B. Li, X. Wei, L. Li and Z. Yang, *Adv. Funct. Mater.* 2013, 23, 970-986.

11 G.-J. Hwang and H. Ohya, *J. Power sources*, 1997, 132, 55-61.

12 J. Xi, Z. Wu, X. Qiu and L. Chen, *J. Power sources*, 2007, 166, 531-536.

13 Z. Mai, H. Zhang, X. Li, S. Xiao and H. Zhang, *J. Power sources*, 2011, 196, 5737-5741.

14 J. Xi, Z. Wu, X. Teng, Y. Zhao, L. Chen and X. Qiu, *J. Mater. Chem.,* 2008, 18, 1232.

15 Q. Luo, H. Zhang, J. Chen, P. Qian and Y. Zhai, *J.Membr. Sci.* 2008, 311, 98-103.

16 J. Zeng, C. Jiang, Y. Wang, J. Chen, S. Zhu, B. Zhao and R. Wang, *Electrochemistry Communications*, 2008, 10, 372-375.

17 G. Decher, *Science*, 1997, 277, 1232-1237.

18 G. Decher, J. D. Hong and J. Schmitt, *Thin Solid Films*, 1992, 210–211, Part 2, 831-835.

19 X. Zhang, H. Chen and H. Zhang, *Chem Commun (Camb)*, 2007, 1395-1405.

20 Y. Wang, S. Wang, M. Xiao, D. Han, M. A. Hickner and Y. Meng, *RSC Adv.*, 2013, 3, 15467.

21 M. Yang, S. Lu, J. Lu, S. P. Jiang and Y. Xiang, *Chem Commun (Camb)*, 2010, 46, 1434-1436.

22 Y. Xiang, S. Lu and S. P. Jiang, *Chem. Soc.Rev.*, 2012, 41, 7291-7321.

23 M. Misono, *Cat. Rev. Sci. Eng.*, 1987, 29, 269-321.

24 X. Teng, J. Dai, J. Su, Y. Zhu, H. Liu and Z. Song, *J. Power sources,* 2013, 240, 131-139.

25 T. Sukkar and M. Skyllas-Kazacos, *J. Appl.Electrochem*, 2004, 34, 137-145.

26 D. Chen, S. Kim, V. Sprenkle and M. A. Hickner, *J. Power sources*, 2013, 231, 301-306.

27 J. Lu, H. Tang, S. Lu, H. Wu and S. P. Jiang, *J. Mater. Chem.*, 2011, 21, 6668.

Figure Captions

Fig.1 Schematic diagram of the Layer-by-Layer self-assembled Nafion-$[CS\text{-}PWA]_n$ membrane

Fig. 2 (a) UV of the Nafion-$[CS\text{-}PWA]_n$ self-assembled membranes**,** (b) FTIR analysis of the pure PWA and CS, and the surface of Nafion-$[CS\text{-}PWA]_3$, measured at room temperature.

Fig.3 AFM images of the membrane surface (a) Nafion membrane, (b) Nafion-$[CS\text{-}PWA]_3$ membrane; SEM and EDX images of the cross-section of the Nafion-$[CS\text{-}PWA]_n$ membrane (c,d and e).

Fig. 4 Plots of (a) conductivity and (b) VO^{2+} permeability of the Nafion membrane as a function of the number of self-assembled CS-PWA multilayer, measured at room temperature.

Fig. 5 Charge-discharge curves of VRFB with Nafion and self-assembled Nafion-$[CS\text{-}PWA]_3$ membranes at 30,40,50,60 mA/cm^2 current density.

Fig. 6 Efficiencies of VRFB with Nafion and self-assembled Nafion-$[CS\text{-}PWA]_3$ membranes at various current densities.

Fig. 7 Open circuit voltage curves of VRFB with Nafion and self-assembled Nafion-$[CS\text{-}PWA]_3$ membranes at *SOC*=80%.

Fig. 8 Cycling performance of efficiency for VRFB with Nafion and self-assembled Nafion-$[CS\text{-}PWA]_3$ membranes at 60 mA/cm^2.

Figures

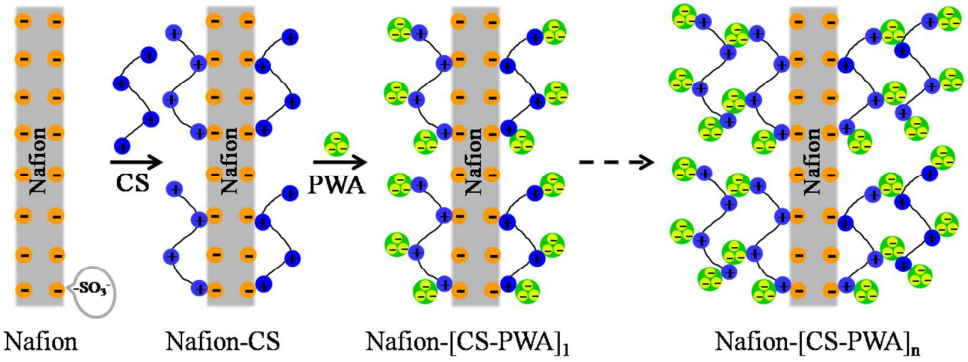

Figure 1

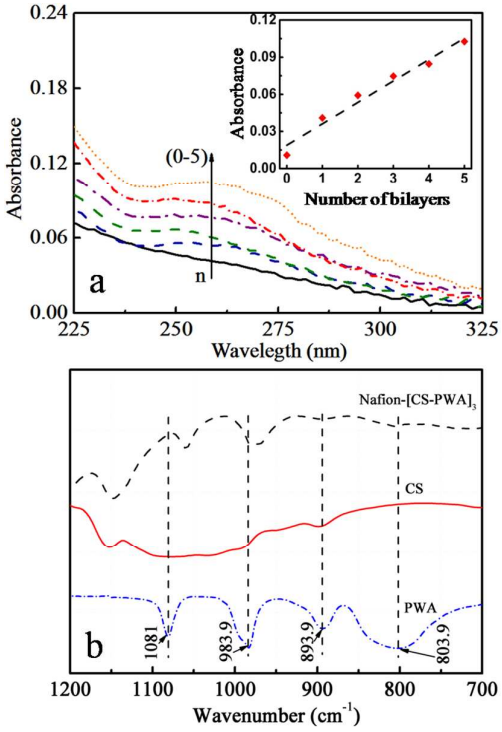

Figure 2

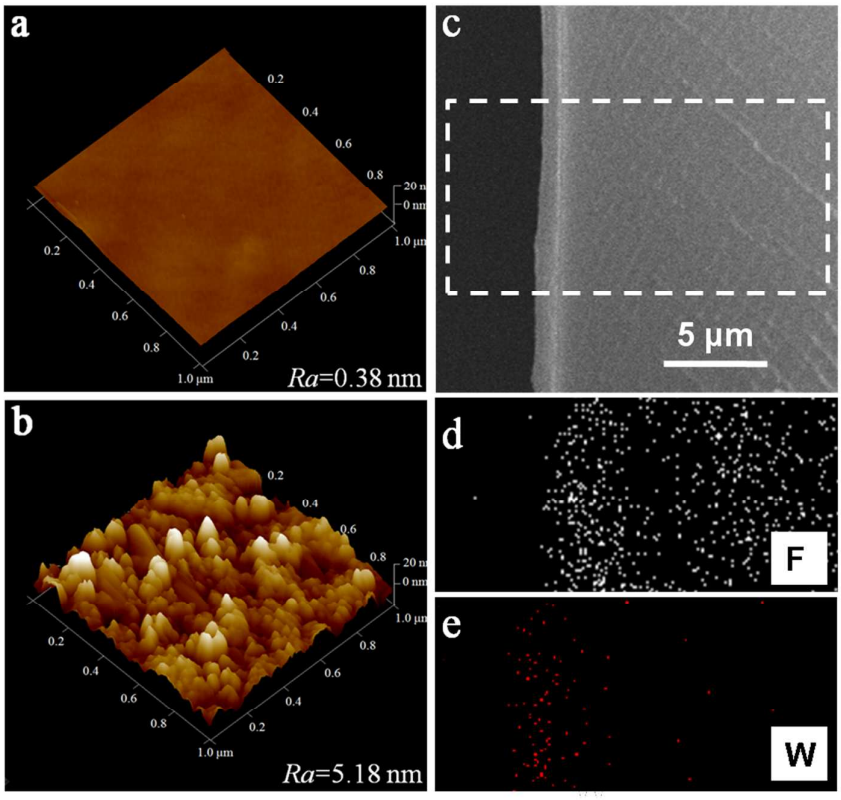

Figure 3

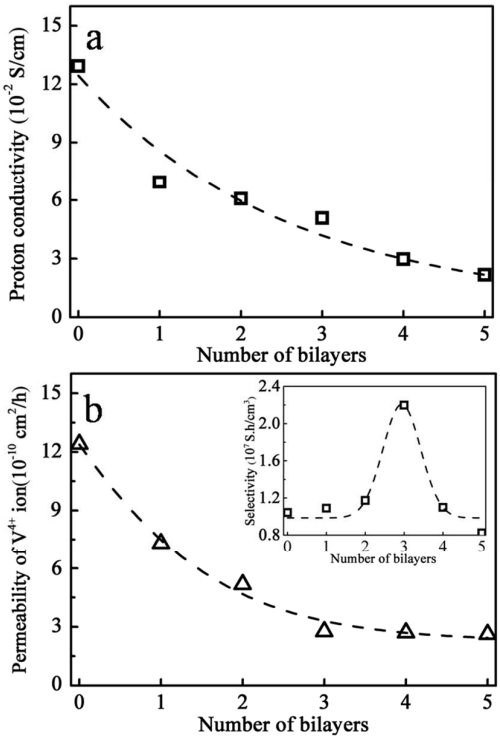

Figure 4

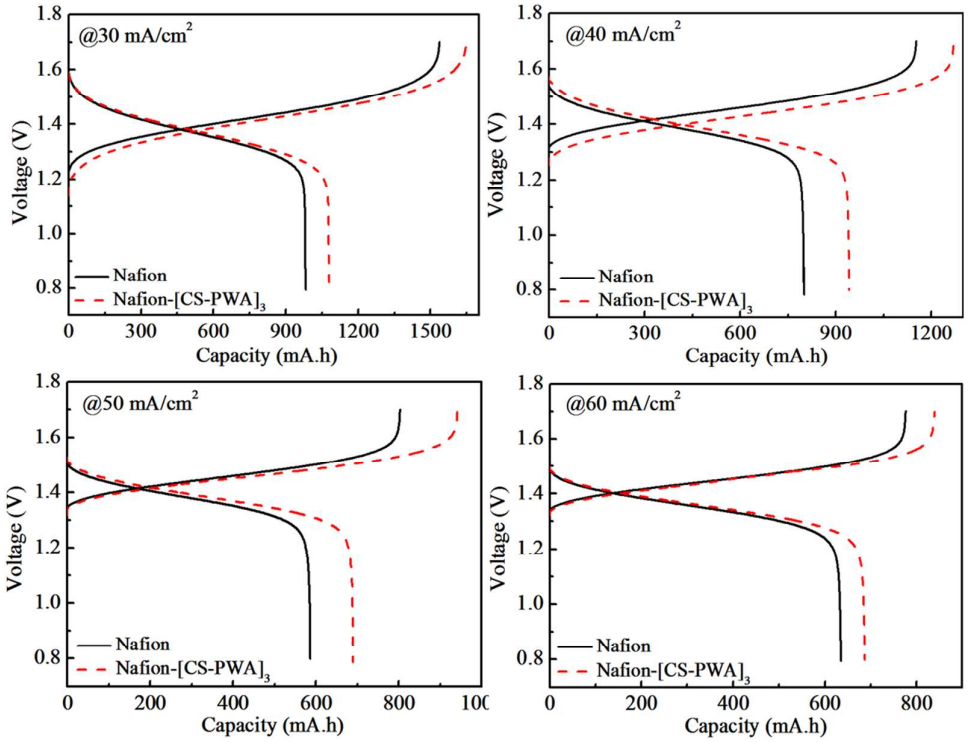

Figure 5

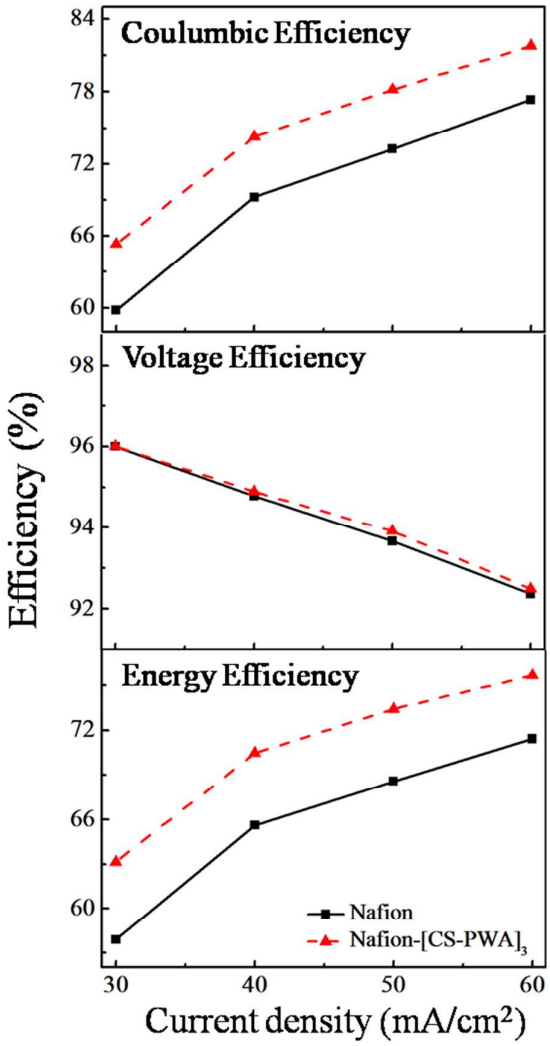

Figure 6

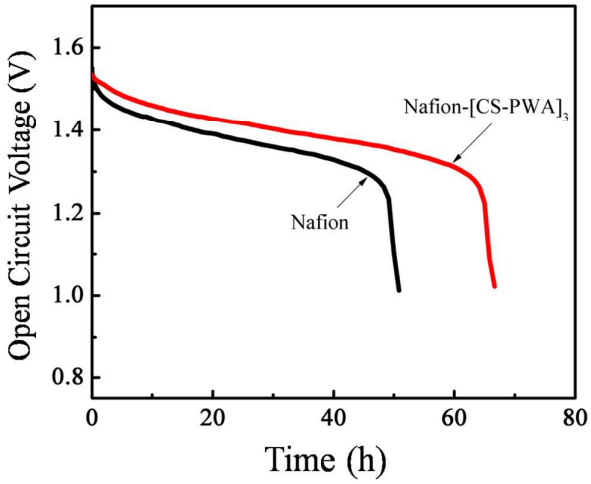

Figure 7

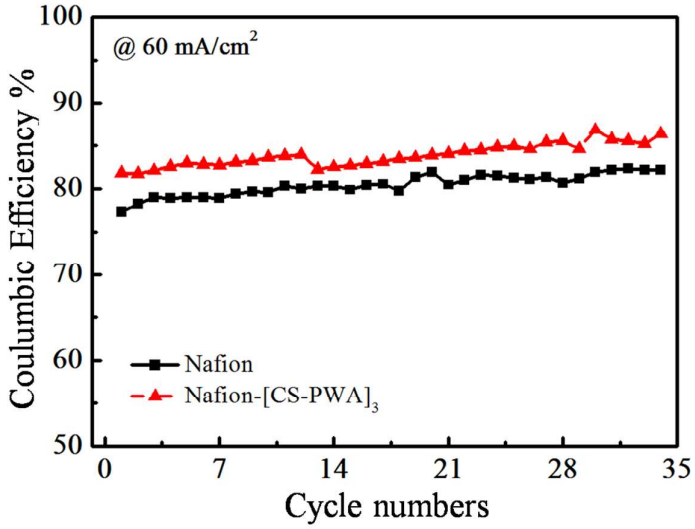

Figure 8